



## Organic–inorganic hybrid membrane with anodized aluminum oxide support layer for improving membrane performance in forward osmosis

Sung Pil Hong<sup>a</sup>, Hongsik Yoon<sup>a</sup>, Choonsoo Kim<sup>a</sup>, Jeyong Yoon<sup>a,b,\*</sup>

<sup>a</sup>*School of Chemical and Biological Engineering, College of Engineering, Institute of Chemical Process, Seoul National University (SNU), Gwanak-gu, Daehak-dong, Seoul 151-742, Korea, Tel. +82-2-880-8941; Fax: +82-2-876-8911; email: jeyong@snu.ac.kr*

<sup>b</sup>*School of Chemical and Biological Engineering, College of Engineering, Institute of Chemical Process, Asian Institute for Energy, Environment & Sustainability (AIEES), Seoul National University (SNU), Gwanak-gu, Daehak-dong, Seoul 151-742, Korea*

Received 6 October 2016; Accepted 16 October 2016

---

### ABSTRACT

In the development of thin-film composite membranes for forward osmosis, the support layer is believed to have a fundamental role, which affects the membrane performance. However, the development of the support layer containing a high surface porosity, straight morphology of pores, and hydrophilic surface has been limited. Here, we report an organic–inorganic hybrid membrane fabricated with an anodized aluminum oxide (AAO) filter as a support layer, which has a high surface porosity, straight pores (tortuosity ~1), and hydrophilic surface. The organic–inorganic hybrid membrane was fabricated by attaching a polyamide thin-selective layer on an AAO filter, which was coated with poly(dopamine). The polyamide thin-selective layer was separated from the polyamide–polysulfone traditional membrane by selectively melting the polysulfone support layer. The membrane performance of the fabricated hybrid membrane was significantly enhanced compared with that of the polyamide–polysulfone membrane because of the diminished salt resistivity by the high surface porosity, unity tortuosity, and surface chemistry of the support layer.

*Keywords:* Forward osmosis; Anodized aluminum oxide; Hybrid membrane

---

### 1. Introduction

An osmotically driven membrane process such as forward osmosis (FO) and pressure retarded osmosis is operated by osmotic pressure across the membrane, which is generated by the difference in the concentration of salts on both sides. Those processes have been regarded as a next generation technology with eco-friendly and energy saving features. The development of membrane technology is key to maximize the membrane performance of osmotically driven processes. Thin-film composite membranes, which consist of an ultrathin selective layer and a support layer, are known for their large potential for osmotically driven membrane processes because their outstanding membrane performance has demonstrated in the reverse osmosis (RO) process [1–3].

The support layer, which provides mechanical strength to the thin-selective layer, possesses a resistivity to the trans-membrane diffusion of salts called dilutive internal concentration polarization (dilutive ICP, Fig. 1) [4–6]. As shown in Fig. 1, when the solute of a draw solution diffuses through the support layer, the diffusion pathway is determined by the thickness and tortuosity, and the total volume of the diffusion pathways is associated with the porosity of the support layer [7]. The long diffusion pathways within the support layer causes delayed salt transport resulting in a significant decrease in the concentration difference across the selective layer (Fig. 1(a)). This dilutive ICP effect significantly reduces the permeation flux by 80% compared with the theoretical value, and has been considered a main obstacle to improving the energy efficiency of the FO process [1,5,8–12]. As shown in Fig. 1(b), designing a thin, less tortuous, and high surface

---

\* Corresponding author.

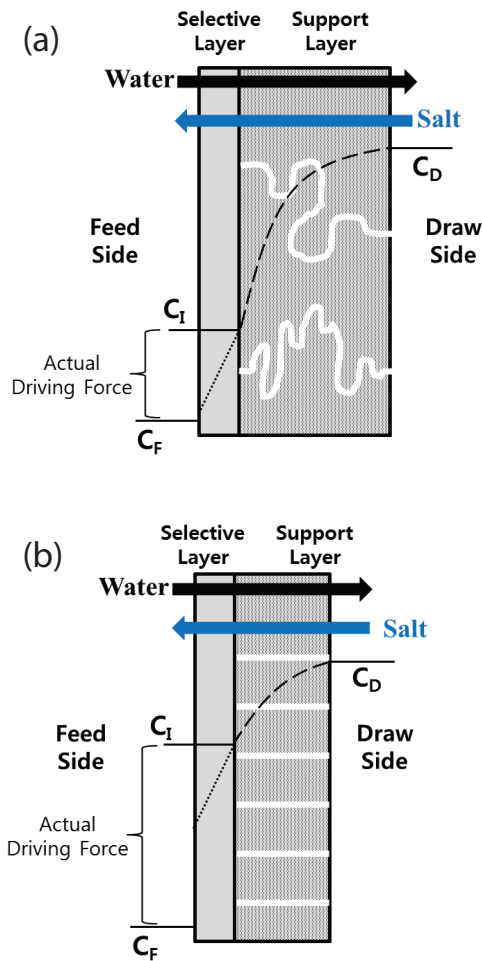


Fig. 1. Concentration profiles of a draw solute in a membrane with different support layer structures. The concentration at interface  $C_I$  between the support and the selective layer of (a) is lower than that of (b) because the support layer of (b) has longer pathways. Because the support layer has a thin thickness, low tortuosity and high porosity, a higher driving force can be obtained across the selective layer (b).  $C_D$  and  $C_F$  are the concentrations at the draw and feed solution, and the dashed black lines are the concentration profiles of the solute. Water is moved by convection, for which the direction is opposite to the direction of salt transport in this system.

porous support layer is necessary as a crucial factor in the development of higher permeation membranes to reduce the resistivity to salt diffusion [4]. Many researchers have reported on improved permeation performance by adjusting the structural characteristics of the support layer; however, the tortuosity issue still remains [2,13,14]. Besides the structural features of the support layer, the chemistry of the support layer has also been of interest as an important factor for improving the permeation flux. For example, the permeation flux was improved by increasing the wettability of a polysulfone (PSf) support layer [15]. A sulfonated polymer was also used to enhance the hydrophilic characteristics of the support layer [16]. However, these conventional approaches are not adequate because they do not provide a high surface

porosity, straight pores (tortuosity  $\sim 1$ ), and hydrophilic characteristics to the support layer.

In this study, the organic–inorganic hybrid membrane, which consisted of an anodized aluminum oxide (AAO) support layer and a polyamide (PA) thin-selective layer, exhibited a high permeation flux and good selectivity due to reduced salt resistivity from the high surface porosity, straight pores, and surface chemistry of the support layer. To fabricate this hybrid membrane, the PA thin-selective layer was separated from the PSf support, which was synthesized by interfacial polymerization on the PSf support layer. The isolated PA thin-selective layer was recombined with a poly(dopamine) coated AAO filter (pAAO) by completely drying them. A poly(dopamine) coating on the support layer could induce a polymer–polymer interaction instead of an organic–inorganic interaction between the two layers [17]. The fabricated PA–pAAO hybrid membrane had enhanced membrane performance compared with that of the conventional PA–PSf membrane. We verified that pAAO support layer reduced the dilutive ICP effect by comparing experimental and structural analyses of the salt resistivity.

## 2. Experimental setup

### 2.1. Synthesis of the polyamide thin-selective layer

The PA thin-selective layer was in situ fabricated by interfacial polymerization on a synthesized PSf support layer. A PA thin-selective layer was synthesized as previously reported procedure [18]. The PSf membrane was immersed in isopropyl alcohol (Aldrich, St. Louis, MO) for 10 min as a pretreatment. After washing with deionized (DI) water, the PSf membrane was placed in a 2 wt% *m*-phenylenediamine (Aldrich, St. Louis, MO) aqueous solution for 3 h. Excess droplets on the wetted PSf membrane were removed by rolling a rubber hand roller, and a 0.1 wt% trimesoyl chloride (Aldrich, St. Louis, MO) solution was poured on the PSf membrane. The interfacial polymerization occurred on the top surface of the PSf support layer, and the reaction time was about 1 min. The synthesized PA–PSf membrane was washed with *n*-hexane solvent (Aldrich, St. Louis, MO) to terminate the reaction, and then, the membrane was dried in an oven at 70°C for 3.5 min. The PA–PSf membrane was stored at 4°C in DI water.

PSf was dissolved in *N*-methyl-2-pyrrolidone (NMP, Aldrich, St. Louis, MO) solvent containing 20 wt% PSf. The PSf membrane was casted by a casting knife with a 150  $\mu\text{m}$  thickness on a polyester nonwoven fabric and put in DI water at room temperature for phase separation.

### 2.2. Fabrication of the organic–inorganic hybrid membrane

The organic–inorganic hybrid membrane was fabricated with a PA thin-selective layer and pAAO support layer. To obtain the PA thin-selective layer, the PA–PSf membrane was put into NMP solvent to melt the PSf support layer. NMP solvent is known as a good swelling solvent for aromatic PA [19]. When only the PA selective layer remained in the NMP solvent, this thin layer was lifted and immersed again in clean NMP solvent for washing. After the washing step, the PA film was placed on a water surface. Because water

has a high surface tension, insoluble PA easily floated on the surface without any wrinkles. Then, the PA film could be scooped up with any substrates as the desired support layer. Here, SUS mesh was applied as substrates as shown in Figs. 2(b)–(d). The PA thin-selective layer was investigated with attenuated total reflectance Fourier transform infrared (ATR-FTIR; Jasco, FT-IR 200) to verify that the amide structures were maintained after dipping in the NMP solvent.

To prepare the pAAO support layer, a commercial AAO filter (Whatman Anodisc, 0.2  $\mu\text{m}$  pore) was coated with poly(dopamine) by the dipping method with phosphate buffer solution containing 2 mg/mL of dopamine (Aldrich, St. Louis, MO) with adjusting pH 8.5 and stationary condition. This pAAO was used to scoop up the PA thin-selective layer on the DI water. The morphology of the fabricated PA–pAAO hybrid membrane was inspected by scanning electron microscopy (SEM, JEOL, JSM-6701F).

### 2.3. Evaluation of membrane performance in the FO process

The evaluation of the membrane performance was done with a lab-scale FO system. DI water and concentrated NaCl solution were used as the feed and draw solution, respectively. To reduce the external pressure effect, the cross-flow velocity was controlled at a very low level of 4 cm/s ( $Re = 234$ ). The operating temperature was room temperature. More details about the FO system are well described in a previous study [20]. The evaluation of the membrane performance for the PA–pAAO hybrid membrane was done after stabilization of the permeation flux. The permeation flux of the membrane was measured by weighing the permeation in the draw side, and reverse salt diffusion was measured with a conductivity meter for 6 L of feed (DI water). The PA–PSf membrane was loaded in the FO process after removing the nonwoven fabric to only consider the effect of the PSf support.

### 2.4. Resistivity analysis of the support layer

The resistivity of the pAAO support layer was estimated by structural and experimental approaches. The resistivity is defined as follows:

$$K = \frac{S}{D} = \frac{t\tau}{D\varepsilon} \quad (1)$$

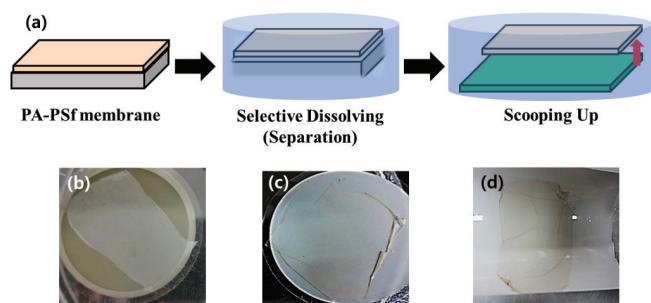


Fig. 2. Scheme showing the basic concept of the fabrication method (a) and photos of products with three different supports (b)–(d). Polyamide thin-selective film was combined with three different support materials, poly(dopamine) coated anodized aluminum oxide filter (b), anodized aluminum oxide filter (c), and polysulfone (d), respectively.

where  $K$  is the salt resistivity for the diffusion within the support layer;  $S$  is the structural factor, and  $D$  is the diffusion coefficient of salts in the solution, which is facing the support layer. The thickness, tortuosity, and porosity of the support layer are represented as  $t$ ,  $\tau$ , and  $\varepsilon$ , respectively. The  $K$  value from Eq. (1) is based on the structure of the support layer. The salt resistivity in the support layer of the PA–pAAO hybrid membrane was calculated from Eq. (1) because pAAO has a regular structure. In most cases, these three structural parameters cannot be easily measured for most polymers. For this reason, the salt resistivity, the  $K$  value, of the support layers was estimated with experimental membrane performance data. The relation between the salt resistivity and experimental membrane performance results is as follows:

$$K = \frac{1}{J_w} \ln \left[ \frac{B + A\pi_{D,b} - J_w}{B + A\pi_{F,b}} \right] \quad (2)$$

where  $J_w$  is the experimental permeation flux;  $A$  is the pure water permeability of a membrane;  $B$  is the salt permeability of a selective layer and  $\pi_{D,b}$  and  $\pi_{F,b}$  are the osmotic pressure of the bulk phase in the draw side and feed side, respectively [5]. The  $A$  and  $B$  parameters were obtained by the dead-end RO test.

## 3. Results

### 3.1. Characterization of the PA selective layer and pAAO support layer

Fig. 3 shows the IR spectrum of the PA thin-selective layer on the PSf support, which was fabricated in the same manner as the fabrication of the organic–inorganic hybrid membrane but with a different support layer (Fig. 2(d)). The typical polyamide peaks remained in this IR spectrum such as the C=O of the amide group at 1,650  $\text{cm}^{-1}$ , the aromatic ring at 1,610  $\text{cm}^{-1}$ , and the C–N of the amide group at 1,540  $\text{cm}^{-1}$  (Figs. 3(a)–(c), respectively). Therefore, no severe degradation of the PA structures occurred during the dissolving of the PSf support layer, which is in agreement with the results of Livingston's group [22]. It is also supported by the retention of the salt rejection property. The salt rejections of the PA thin-selective layers on the PSf support and on the pAAO support layer (before and after the dissolving process, respectively) were measured by the RO test, which was done in a dead-end cell at 600 rpm (data not shown).

Fig. 4 shows the structures of the AAO, pAAO, and hybrid membrane. As shown in Figs. 4(a)–(d), no significant changes in the AAO structure were observed from the poly(dopamine) coating. The porosities of the front side of the AAO and pAAO were 53%  $\pm$  0.8% and 51%  $\pm$  2.3% as shown in Figs. 4(a) and (c), respectively. The porosities of the back side were likewise similar at 53%  $\pm$  1.0% for the AAO and 51%  $\pm$  0.9% for the pAAO (Figs. 4(b) and (d)), and all porosity values were calculated with the ImageJ software. The unchanged porosity of the AAO and pAAO implies that the pore size and thickness were not significantly affected by the poly(dopamine) coating. Therefore, the salt resistivity of the support layer could be maintained despite the poly(dopamine) coating. The top of the pAAO support layer

was well covered with the PA thin-selective layer in Fig. 4(e), which was transferred from the PSf support to the pAAO

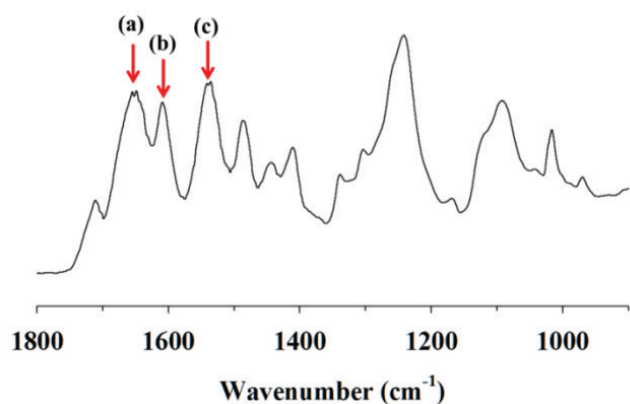


Fig. 3. ATR-IR spectrum of the polyamide after selectively dissolving the polysulfone support layer. Amide C=O peak at  $1650\text{ cm}^{-1}$  (a), aromatic ring peak at  $1610\text{ cm}^{-1}$  (b) and amide C–N peak at  $1540\text{ cm}^{-1}$  (c) [8,21]. This IR spectrum was from the polyamide thin-selective layer recombined with the polysulfone support layer. The typical amide bond of the polyamide thin-selective layer remained after the selective dissolving process.

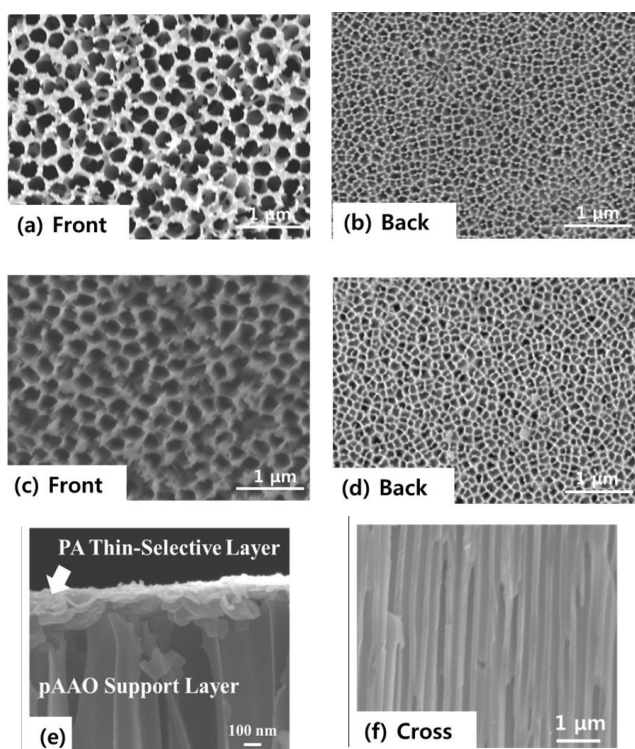


Fig. 4. SEM images of the anodized aluminum oxide (AAO) filters without the poly(dopamine) coating (a) and (b), with coating (c) and (d), and the organic–inorganic hybrid membrane (e) and (f): front and back side of the bare AAO (a) and (b), and front and back side of the poly(dopamine) coated AAO (c) and (d). The morphology between the bare and coated AAO was almost the same. Straight channels are seen in the cross-section image (f), which reflect the unity tortuosity. The porosity of the coated AAO was 46%, which was measured with the ImageJ software.

support layer. As shown in Fig. 4(f), there were straight pores (unity tortuosity) in cross-section image, which was a unique characteristic of the AAO material.

### 3.2. Evaluation of the PA–pAAO hybrid membrane performance in the FO process

The PA–pAAO hybrid membrane was evaluated in the FO system. Fig. 5 shows the performance evaluation results of the three different membranes. The permeation flux of the PA–pAAO ( $65\text{ L/m}^2\text{h}$ ) was enhanced dramatically compared with the hand-casted and commercial PA–PSf membranes ( $5.2$  and  $11\text{ L/m}^2\text{ h}$ , respectively). This improvement was caused by minimizing the ICP effect due to the straight pores and hydrophilic surface of the pAAO support layer. The permeation flux of the hand-casted PA–PSf was less than that of the commercial PA–PSf because the thicker support layer of the hand-casted PA–PSf results in a higher resistivity to salt diffusion of the support layer. The selectivity of the PA–pAAO was one order of magnitude higher than that of the commercial PA–PSf ( $\sim 600$  and  $\sim 40\text{ L/mol}$ , respectively). The selectivity could be estimated from the ratio of the permeation flux to the reverse salt diffusion flux in the FO process. The enhanced permeation flux and high selectivity were caused by a large difference in the salt concentration across the PA selective thin-layer, which occurred due to the pAAO support layer by the increased accessibility of the draw solution to the PA selective thin-layer.

### 3.3. Estimation of the salt diffusion resistivity ( $K$ value) of the support layers

The resistivity of the salt diffusion of the pAAO support layer was estimated (Table 1). Membrane performance can be affected by the structural features of its support layer, which can be shown by the resistivity ( $K$  value) of the salt diffusion.

The  $K$  values are presented in Table 1. The  $K$  values of the PA–pAAO and PA–PSf membranes were calculated as

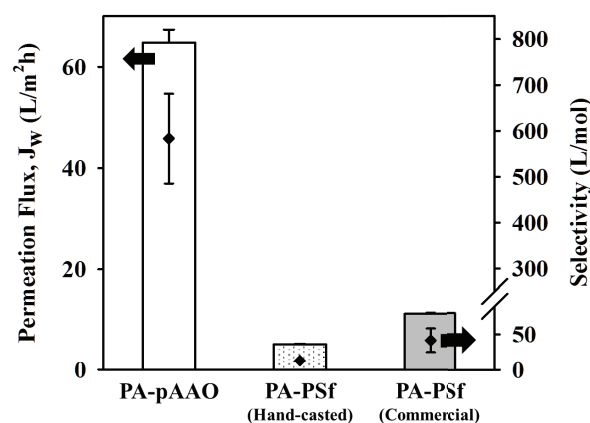


Fig. 5. Permeation flux and selectivity of forward osmosis membranes evaluated with a  $1\text{ M NaCl}$  draw solution. The hand-casted PA–PSf was synthesized in a laboratory, which was the source of PA thin-selective layer on the pAAO support. Selectivity (diamond marks) was the ratio of the permeation flux ( $\text{L/m}^2\text{ h}$ ) to reverse salt diffusion ( $\text{mol/m}^2\text{ h}$ ).

Table 1  
Comparison of the support layer resistivity ( $K$  value) based on the support layer

	Permeation flux (L/m <sup>2</sup> h)	Resistivity, $K$ value (10 <sup>5</sup> s/m)
PA-pAAO	30.9	1.3 <sup>a</sup>
	39 <sup>b</sup>	0.84 <sup>c</sup>
PA-PSf without fabric	5.05	16

<sup>a</sup>Calculated value from Eq. (2).

<sup>b</sup>Expected value of the resistivity calculated from Eq. (1).

<sup>c</sup>Calculated value from Eq. (1).

$1.30 \times 10^5$  and  $1.62 \times 10^6$  s/m from Eq. (2), respectively, which means that the pAAO support layer has a lower salt resistivity for diffusion in the support layer. However, the  $K$  value of the AAO from the structural characteristics, Eq. (1), was  $8.4 \times 10^4$  s/m, and the prediction flux based on this salt resistivity for diffusion was about 39 L/m<sup>2</sup> h. This gap between the  $K$  values from Eqs. (1) and (2) implies that other factors in addition to the ICP may contribute to determining the permeation performance; however, this effect could be negligible when comparing the difference between the  $K$  values of the PA-pAAO and PA-PSf without fabric. Additionally, Eq. (1) has not been applied except to the AAO support layer because the structural parameters for this equation could not be measured directly. However, the pAAO has a well-defined structure. For this reason, the experimental  $K$  value for the PA-pAAO could be verified with this structural approach.

#### 4. Conclusion

The organic-inorganic hybrid membrane PA-pAAO exhibited highly enhanced permeation and high selectivity compared with the PA-PSf membrane. The results of the estimation for the salt resistivity for diffusion in the support layer confirmed that the dilutive ICP effect was significantly reduced when AAO was used as a support layer due to its structural features including its high surface area and unity tortuosity. In addition, the approach, in which the selective layer and the support layer are handled separately, can be used for analytic methods to investigate the selective layer and the support layer independently.

#### Acknowledgments

This research was supported by a grant (code 13IFIP-B065893-01) from the Industrial Facilities and Infrastructure Research Program funded by the Ministry of Land, Infrastructure and Transport of the Korean Government. This subject is supported by Korea Ministry of Environment as "Global Top Project (E616-00211-0608-0)".

#### References

- [1] N.Y. Yip, A. Tiraferri, W.A. Phillip, J.D. Schiffman, M. Elimelech, High performance thin-film composite forward osmosis membrane, *Environ. Sci. Technol.*, 44 (2010) 3812–3818.

- [2] K.Y. Wang, T.S. Chung, G. Amy, Developing thin-film-composite forward osmosis membranes on the PES/SPSf substrate through interfacial polymerization, *AIChE J.*, 58 (2012) 770–781.
- [3] G. Han, S. Zhang, X. Li, N. Widjojo, T.-S. Chung, Thin film composite forward osmosis membranes based on polydopamine modified polysulfone substrates with enhancements in both water flux and salt rejection, *Chem. Eng. Sci.*, 80 (2012) 219–231.
- [4] G.T. Gray, J.R. McCutcheon, M. Elimelech, Internal concentration polarization in forward osmosis: role of membrane orientation, *Desalination*, 197 (2006) 1–8.
- [5] J.R. McCutcheon, M. Elimelech, Influence of concentrative and dilutive internal concentration polarization on flux behavior in forward osmosis, *J. Membr. Sci.*, 284 (2006) 237–247.
- [6] C.Y. Tang, Q. She, W.C.L. Lay, R. Wang, A.G. Fane, Coupled effects of internal concentration polarization and fouling on flux behavior of forward osmosis membranes during humic acid filtration, *J. Membr. Sci.*, 354 (2010) 123–133.
- [7] K. Lee, R. Baker, H. Lonsdale, Membranes for power generation by pressure-retarded osmosis, *J. Membr. Sci.*, 8 (1981) 141–171.
- [8] N.-N. Bui, M.L. Lind, E.M.V. Hoek, J.R. McCutcheon, Electrospun nanofiber supported thin film composite membranes for engineered osmosis, *J. Membr. Sci.*, 385–386 (2011) 10–19.
- [9] X. Song, Z. Liu, D.D. Sun, Nano gives the answer: breaking the bottleneck of internal concentration polarization with a nanofiber composite forward osmosis membrane for a high water production rate, *Adv. Mater.*, 23 (2011) 3256–3260.
- [10] R. Wang, L. Shi, C.Y. Tang, S. Chou, C. Qui, A.G. Fane, Characterization of novel forward osmosis hollow fiber membranes, *J. Membr. Sci.*, 355 (2010) 158–167.
- [11] S. Zhang, K.Y. Wang, T.-S. Chung, Hchen, Y. Jean, G. Amy, Well-constructed cellulose acetate membranes for forward osmosis: minimized internal concentration polarization with an ultra-thin selective layer, *J. Membr. Sci.*, 360 (2010) 522–535.
- [12] J. Wei, C. Qui, C.Y. Tang, R. Wang, A.G. Fane, Synthesis and characterization of flat-sheet thin film composite forward osmosis membranes, *J. Membr. Sci.*, 372 (2011) 292–302.
- [13] A. Tiraferri, N.Y. Yip, W.A. Phillip, J.D. Schiffman, M. Elimelech, Relating performance of thin-film composite forward osmosis membranes to support layer formation and structure, *J. Membr. Sci.*, 367 (2011) 340–352.
- [14] G. Han, T.-S. Chung, M. Toriida, S. Tamai, Thin-film composite forward osmosis membranes with novel hydrophilic supports for desalination, *J. Membr. Sci.*, 423–424 (2012) 543–555.
- [15] J.R. McCutcheon, M. Elimelech, Influence of membrane support layer hydrophobicity on water flux in osmotically driven membrane processes, *J. Membr. Sci.*, 318 (2008) 458–466.
- [16] N. Widjojo, T.-S. Chung, M. Weber, C. Maletzko, V. Warzelhan, The role of sulfonated polymer and macrovoid-free structure in the support layer for thin-film composite (TFC) forward osmosis (FO) membranes, *J. Membr. Sci.*, 383 (2011) 214–223.
- [17] H. Lee, N.F. Scherer, P.B. Messersmith, Single-molecule mechanics of mussel adhesion, *Proc. Natl. Acad. Sci. USA*, 103 (2006) 12999–13003.
- [18] H.J. Kim, K. Choi, Y. Baek, D.-G. Kim, J. Shim, J. Yoon, J.-C. Lee, High-performance reverse osmosis CNT/polyamide nanocomposite membrane by controlled interfacial interactions, *ACS Appl. Mater. Interfaces*, 6 (2014) 2819–2829.
- [19] V. Freger, Swelling and morphology of the skin layer of polyamide composite membranes: an atomic force microscopy study, *Environ. Sci. Technol.*, 38 (2004) 3168–3175.
- [20] H. Yoon, Y. Baek, J. Yu, J. Yoon, Biofouling occurrence process and its control in the forward osmosis, *Desalination*, 325 (2013) 30–36.
- [21] J. Yu, Y. Baek, H. Yoon, J. Yoon, New disinfectant to control biofouling of polyamide reverse osmosis membrane, *J. Membr. Sci.*, 427 (2013) 30–36.
- [22] S. Karan, Z. Jiang, A.G. Livingston, Sub-10 nm polyamide nanofilms with ultrafast solvent transport for molecular separation, *Science*, 348 (2015) 1347–1351.